



A truly boundary-only meshfree method for inhomogeneous problems based on recursive composite multiple reciprocity technique

W. Chen ^{*}, Z.J. Fu, B.T. Jin

Center for Numerical Simulation Software in Engineering and Sciences, Department of Engineering Mechanics, College of Civil Engineering, Hohai University, No. 1 XiKang Road, Nanjing, Jiangsu 210098, China

ARTICLE INFO

Article history:

Received 15 May 2009

Accepted 27 September 2009

Keywords:

Boundary particle method
Recursive composite multiple reciprocity
Meshfree
Boundary only
Inhomogeneous problems
High-order harmonic solutions

ABSTRACT

This study presents a novel technique called the recursive composite multiple reciprocity method (RC-MRM), to develop a truly boundary-only meshfree boundary particle method (BPM) for general inhomogeneous problems. It does not require any inner nodes to evaluate the particular solution, and thus it is a truly boundary-only numerical method. “Composite” in the RC-MRM implies that the RC-MRM employs a high-order composite differential operator rather than a high-order Laplacian operator in the standard MRM to annihilate inhomogeneous term of various types and enables the present BPM to handle a much wider variety of inhomogeneous problems, while the “recursive” algorithm in the RC-MRM significantly reduces CPU time and storage requirements of the original MRM. In addition, we also find high-order harmonic solutions of the Laplacian operator. Numerical illustrations reveals that the present BPM has rapid convergence, high accuracy and efficiency, and mathematical simplicity, through various two- and three-dimensional benchmark problems.

© 2009 Published by Elsevier Ltd.

1. Introduction

Recent decades have witnessed a research boom on meshfree numerical partial differential equation (PDE) techniques since mesh generation in the standard finite element method (FEM) and boundary element method (BEM) is not trivial, especially for high-dimensional moving boundary problems. This study focuses on the boundary-type meshfree numerical techniques relative to the mesh-based BEM. Among the representative methods of this type are boundary node method (BNM) [1], local boundary integral equation method (LBIEM) [2], boundary cloud method (BCM) [3], boundary point method [4], method of fundamental solutions (MFS) [5,6], and boundary knot method (BKM) [7,8]. The essence of all these techniques, except MFS and BKM, is basically a combination of the moving least square (MLS) technique with various boundary element schemes. These MLS-based boundary meshfree methods involve singular integration and require shadow background meshes for numerical integrations. Hence they are mathematically complicated and computationally very expensive.

In contrast, the MFS and the BKM possess integration-free, spectral convergence, easy-to-use and inherently meshfree, and are thus very efficient and accurate. However, the MFS [5] requires

a fictitious boundary outside the physical domain to avoid singularities of the fundamental solution. This fictitious boundary can be arbitrary and makes the method less feasible for complex-shaped and multiply connected domain problems. On the other hand, the BKM uses the nonsingular general solution instead of the singular fundamental solution and thus circumvents the controversial artificial boundary in the MFS. But not all differential equations have nonsingular general solutions, for instance, Laplace equation. Hon and Wu [9] applied the translation-invariant two dimensional (2D) Laplacian nonsingular harmonic function for solving Laplace problems. In this study, we extend the application of the Laplacian harmonic function to three-dimensional (3D) problems and introduce high-order harmonic functions in the BPM.

In the past decade, the dual reciprocity method (DRM) [10,11] and multiple reciprocity method (MRM) [11,12] have been emerging as the two most promising techniques to handle inhomogeneous term in conjunction with the boundary-type methods [13–15]. For instance, the so-called DR-BEM and MR-BEM are very popular in the BEM community. The DRM has become de facto the method of choice in the boundary-type methods to evaluate the particular solution, since it is easier to use, more efficient, and more flexible to handle a variety of problems. However, the DRM demands inner nodes to guarantee convergence and stability in the calculation of the particular solution. Therefore, these methods are not truly boundary-only as their names may imply.

^{*} Corresponding author. Tel.: +86 25 83786873; fax: +86 25 83736860.
E-mail address: chenwen@hhu.edu.cn (W. Chen).

It is claimed that the MRM has the striking advantage over the DRM in that it does not require inner nodes at all for inhomogeneous problems. To take advantage of the MRM truly boundary-only merit, Chen [16] recently developed the MRM-based meshfree boundary particle method (BPM). However, the MRM also has some disadvantages compared with the DRM in that the standard MRM is computationally much more expensive in the construction of different interpolation matrices and has limited feasibility for general inhomogeneous problems due to its conventional use of high-order Laplacian operators in the annihilation process.

This study proposes a recursive composite multiple reciprocity (RC-MRM) technique to tackle these drawbacks of the MRM in the BPM. “Composite” implies that the RC-MRM employs a high-order composite differential operator rather than a high-order Laplacian operator in the standard MRM to annihilate inhomogeneous term of various types, which enables the present BPM to handle a much wider variety of inhomogeneous problems, while the “recursive” algorithm in the RC-MRM significantly reduces CPU time and storage requirements of the original MRM. The BPM based on the RC-MRM is thus a truly boundary-only numerical technique for inhomogeneous problems. Section 2 introduces the recursive composite multiple reciprocity method, followed by numerical validations of its efficiency in terms of some 2D and 3D Poisson- and Helmholtz-type problems in Section 3. Section 4 concludes this paper with discussions of the potential applicability and opening issues of the present method.

2. Recursive composite multiple reciprocity technique

When the boundary-type numerical method is applied to inhomogeneous problems, the solution is usually split into homogeneous and particular solutions. To clearly illustrate the approach, consider the following example without loss of generality:

$$\mathfrak{R}\{u\} = f(x), \quad x \in \Omega \tag{1}$$

$$u(x) = R(x), \quad x \subset \Gamma_D \tag{2a}$$

$$\frac{\partial u(x)}{\partial n} = N(x), \quad x \subset \Gamma_N \tag{2b}$$

where \mathfrak{R} is a differential operator, x means a multi-dimensional independent variable, Γ_D and Γ_N are the Dirichlet and Neumann boundary parts, respectively, and n the unit outward normal. The solution of Eq. (1) can be expressed as

$$u = u_h + u_p \tag{3}$$

where u_h and u_p are the homogeneous and the particular solutions, respectively. The particular solution u_p satisfies

$$\mathfrak{R}\{u_p\} = f(x) \tag{4}$$

but does not necessarily satisfy boundary conditions. In contrast, the homogeneous solution has to satisfy not only the corresponding homogeneous equation

$$\mathfrak{R}\{u_h\} = 0 \tag{5}$$

but also boundary conditions

$$u_h(x) = R(x) - u_p(x), \quad x \in \Gamma_D \tag{6a}$$

$$\frac{\partial u_h(x)}{\partial n} = N(x) - \frac{\partial u_p(x)}{\partial n}, \quad x \in \Gamma_N \tag{6b}$$

The homogeneous solution u_h from Eqs. (5) and (6) can be efficiently calculated by the boundary-type numerical techniques with the fundamental solution [17,18], general solution

[16,18], Trefftz function [19,20], and de-singular fundamental solution [21].

To evaluate the particular solution u_p , we use a novel technique, the recursive composite multiple reciprocity method, to cure these perplexing problems while keeping the merits of the MRM being truly boundary-only, and overcome the major drawbacks about limited applicability and high computational cost in the MRM.

“Composite” in the RC-MRM implies that the annihilating differential operator in the MRM is not necessary $\mathfrak{R}\{ \}$ in the governing equation (1). Instead, a composite differential operator can be chosen to realize the basic assumption of the MRM, vanishing the inhomogeneous term $f(x)$ in Eq. (1) by iterative differentiations

$$\lim_{m \rightarrow \infty} L_m \dots L_2 L_1 \{f(x)\} \rightarrow 0 \tag{7}$$

where L_1, L_2, \dots, L_m are differential operators of the same kind or different kinds. Unlike the original MRM, the iterative annihilating differential operator in (7) is not restricted to the same one of the governing equation, i.e. Laplacian operators. Comparing the above composite MRM (7) with the original MRM we can see that (7) has greater flexibility and wider applicability to embrace the features of inhomogeneous function $f(x)$. Under the assumption that the annihilation (7) is finite order or is truncated at certain order M , we have the composite MRM equation

$$L_M \dots L_2 L_1 \mathfrak{R}\{u\} \cong 0, \quad x \in \Omega \tag{8}$$

This is a high-order homogeneous equation underlying the original inhomogeneous governing equation (1). The solution procedure of the composite MRM is similar to the one in the original MRM. Thus, Eq. (1) is transformed into a higher-order homogeneous equation as given by Eq. (8). In order that Eq. (8) has a unique solution, $M+1$ boundary conditions must be supplied. We consider the following boundary conditions apart from that given by Eq. (2):

$$\begin{cases} \mathfrak{R}u(x) = f(x), & x \in \partial\Omega \\ L_1 \mathfrak{R}u(x) = L_1 f(x), & x \in \partial\Omega \\ \vdots \\ L_{M-1} \dots L_2 L_1 \mathfrak{R}u(x) = L_{M-1} \dots L_1 f(x), & x \in \partial\Omega \end{cases} \tag{9}$$

Therefore the inhomogeneous problem (1) and (2) is reduced to a homogeneous higher-order elliptic partial differential problem (8) subjected to the boundary conditions given by Eqs. (2) and (9). Thus, the present BPM can also use the fundamental solution, general solution, T-function, and de-singular fundamental solution as the approximate basis functions, to evaluate the homogeneous solution of the above transformed equation via only boundary discretization.

In this section we choose the singular fundamental solution to illustrate the present BPM solution procedure. The BPM approximates the solution by a linear combination of singular fundamental solutions, i.e., the approximate solution $u(x)$ given by [14]

$$u(x) = \sum_{i=0}^M \sum_{j=1}^{n_s} a_{ij} u_i^*(x - y_j) = \sum_{i=0}^M \hat{u}_i \tag{10}$$

where a_{ij} are unknown coefficients to be determined, and y_j are source points located on a fictitious boundary outside the solution domain. The function $u_i^*(x)$ is the fundamental solution of the composite operator L_j , and a higher-order fundamental solution is employed if it occurs repetitively. Homogeneous

solutions \hat{u}_i are defined as follows:

$$\hat{u}_i = \sum_{j=1}^{n_s} a_{ij} u_i^*(x - y_j), \quad i = 0, 1, 2, \dots, M \quad (11)$$

In order to solve the higher-order homogeneous problem efficiently, we derive a recursive procedure in the following. First recall the following important property of the fundamental solutions:

$$\Re u_0(x) = \delta(x), \quad (12a)$$

$$L_i u_i(x) = \delta(x), \quad i = 1, 2, \dots, M \quad (12b)$$

where $\delta(x)$ is the Dirac delta function. Therefore we have

$$\Re u_0(x - y_j) = \delta(x - y_j), \quad j = 1, 2, \dots, n_s \quad (13a)$$

$$L_i u_i(x - y_j) = \delta(x - y_j), \quad j = 1, 2, \dots, n_s \quad (13b)$$

since the source points y_j are placed on a fictitious boundary outside the solution domain, $L_i u_i(x)$ vanishes identically on the physical boundary Ω . Inserting Eq. (10) into Eqs. (2) and (9) and taking into consideration Eq. (8), we have

$$\left\{ \begin{array}{l} \sum_{i=0}^M \hat{u}_i(x) = R(x), \quad x \in \Gamma_D \\ \frac{\partial}{\partial n} \sum_{i=0}^M \hat{u}_i(x) = N(x), \quad x \in \Gamma_N \\ \Re \sum_{i=1}^M \hat{u}_i(x) = f(x), \quad x \in \partial\Omega \\ L_1 \Re \sum_{i=2}^M \hat{u}_i(x) = L_1 f(x), \quad x \in \partial\Omega \\ \vdots \\ L_{M-1} \cdots L_2 L_1 \Re \hat{u}_M(x) = L_{M-1} \cdots L_1 f(x), \quad x \in \partial\Omega \end{array} \right. \quad (14)$$

Let x_k be L collocation points chosen along the boundary. By collocating Eq. (14) at these boundary collocation points x_k , we arrive at the following system of linear equations:

$$\left\{ \begin{array}{l} \mathbf{A}_{00} \mathbf{a}_0 + \mathbf{A}_{01} \mathbf{a}_1 + \cdots + \mathbf{A}_{1M} \mathbf{a}_M = \mathbf{b}_0 \\ \mathbf{A}_{11} \mathbf{a}_1 + \cdots + \mathbf{A}_{1M} \mathbf{a}_M = \mathbf{b}_1 \\ \vdots \\ \mathbf{A}_{MM} \mathbf{a}_M = \mathbf{b}_M \end{array} \right. \quad (15a)$$

where a_i are unknown coefficient vectors to be determined:

$$\mathbf{a}_i = (a_{i1}, a_{i2}, \dots, a_{in_s})^T, \quad i = 0, 1, 2, \dots, M \quad (15b)$$

b_i are the known data vector defined as

$$\left\{ \begin{array}{l} \mathbf{b}_0 = (R(x_1), R(x_2), \dots, R(x_{n_1}), N(x_{n_1+1}), \dots, N(x_L))^T \\ \mathbf{b}_i = (f_i(x_1), f_i(x_2), \dots, f_i(x_L))^T, \quad i = 1, 2, \dots, M \end{array} \right. \quad (15c)$$

where

$$f_i(x) = L_{i-1} \cdots L_2 L_1 f(x) \quad (15d)$$

and A_{ij} are interpolation matrices:

$$\mathbf{A}_{0j} = \begin{cases} u_j(x_l - y_m), & l = 1, 2, \dots, n_1, \quad m = 1, 2, \dots, n_s \\ \frac{\partial}{\partial n} u_j(x_l - y_m), & l = n_1 + 1, \dots, L, \quad m = 1, 2, \dots, n_s \end{cases}, \quad j = 0, 1, 2, \dots, M \quad (15e)$$

$$\mathbf{A}_{ij} = L_{i-1} \cdots L_2 L_1 u_j(x_l - y_m), \quad l = 1, 2, \dots, n_1, \quad m = 1, 2, \dots, n_s, \quad i = 1, 2, \dots, M, \quad j = 1, 2, \dots, M \quad (15f)$$

“Recursive” in the RC-MRM implies that the system (15a) can be conveniently solved using a recursively procedure

$$\mathbf{a}_M \rightarrow \mathbf{a}_{M-1} \rightarrow \cdots \rightarrow \mathbf{a}_1 \rightarrow \mathbf{a}_0 \quad (16)$$

Therefore, the computational effort does not generally grow much with respect to the increasing number of the differential operators to annihilate the forcing term.

There are a few properties that can be utilized to reduce the computational effort in generating the interpolation matrix. For example, when a differential operator occurs repetitively, their respective interpolation matrices are the same if the higher-order fundamental are chosen appropriately. In the case of that the operator $\Re = L_1 = L_2$, the fundamental solutions $u_0^*(x)$, $u_1^*(x)$ and $u_2^*(x)$ such that $L u_1^*(x) = u_0^*(x)$ and $L u_2^*(x) = u_1^*(x)$ hold; then we have the useful property $\mathbf{A}_{11} = \mathbf{A}_{22}$ irrespective of the boundary conditions. For the Dirichlet boundary condition, we have $\mathbf{A}_{00} = \mathbf{A}_{11} = \mathbf{A}_{22}$, and $\mathbf{A}_{01} = \mathbf{A}_{12}$.

It is stressed that throughout the solution procedure of the present recursive composite multiple reciprocity method, we do not use any inner nodes. In particular, the algorithm is novel in using a composite high-order differential operator to smooth out the inhomogeneous term without increasing computing efforts. The essential differences between the present RC-MRM and the standard MRM can be summarized by two aspects: (1) differential operators different from the governing differential operator may also be employed to annihilate the inhomogeneous term and (2) the recursive algorithm is used to reduce computing cost dramatically.

3. Numerical results and discussion

In this section we present several numerical examples to illustrate the efficiency and stability of the proposed method for several inhomogeneous boundary value problems, and they are compared with results reported in the literature. Numerical results for 2D and 3D Poisson- and Helmholtz-type problems are presented.

The average relative error $rerr(u)$, average absolute error $aerr(u)$ and maximum error $merr(u)$ defined as follows are used to measure the accuracy of the numerical results:

$$rerr(u) = \sqrt{\frac{\sum_{k=1}^N (u_k - \tilde{u}_k)^2}{\sum_{k=1}^N (u_k)^2}} \quad (17a)$$

$$aerr(u) = \sqrt{\frac{1}{N} \sum_{k=1}^N (u_k - \tilde{u}_k)^2} \quad (17b)$$

$$merr(u) = \max_k |u_k - \tilde{u}_k| \quad (17c)$$

where u_k and \tilde{u}_k are the analytical and numerical solutions evaluated at x_k , respectively, and N is the total number of evaluated points. Unless otherwise specified, N is taken to be 10,000 for 2D problems and 27,000 for 3D problems for the numerical results presented below, which are evenly distributed in the domain and on the boundary. In all numerical computations, the number of source points is taken to be equal to that of boundary collocation points.

3.1. BPM with singular formulation

Example 1. (Polynomial forcing term) First we consider the Poisson’s equation with a polynomial forcing term

$$\begin{cases} \Delta u = -x_1^2, & (x_1, x_2) \in \Omega \\ u = 0, & (x_1, x_2) \in \partial\Omega \end{cases} \quad (18a)$$

where Ω is an ellipse with a semi-major axis of length 2 and semi-minor axis of length 1. The exact solution is given by [10]

$$u(x) = -\frac{1}{246}(50x_1^2 - 8x_2^2 + 33.6)\left(\frac{x_1^2}{4} + x_2^2 - 1\right) \quad (18b)$$

For this example, the proposed method solves the following homogeneous problem:

$$\begin{cases} \Delta^3 u = 0, & (x_1, x_2) \in \Omega \\ u = 0, & (x_1, x_2) \in \partial\Omega \\ \Delta u = -x_1^2, & (x_1, x_2) \in \partial\Omega \\ \Delta^2 u = -2, & (x_1, x_2) \in \partial\Omega \end{cases} \quad (18c)$$

The fundamental solutions $u_1^*(x)$, $u_2^*(x)$, and $u_3^*(x)$ to the differential operators \mathfrak{R} , L_1 and L_2 are given by [17]

$$\begin{aligned} u_1^*(x) &= -\frac{1}{2\pi} \ln r, & u_2^*(x) &= -\frac{1}{8\pi} r^2 \ln r, \\ u_3^*(x) &= -\frac{1}{128\pi} r^4 \ln r \end{aligned} \quad (18d)$$

Note that u_1^* and u_2^* are taken to be higher-order fundamental solutions to the 2D Laplacian, since the differential operators $\mathfrak{R} = L_1 = L_2$.

To implement the BPM with singular formulation, Fig. 1 shows the source points located on an ellipse with a semi-major axis length of 10 and semi-minor axis length of 5 centered at the

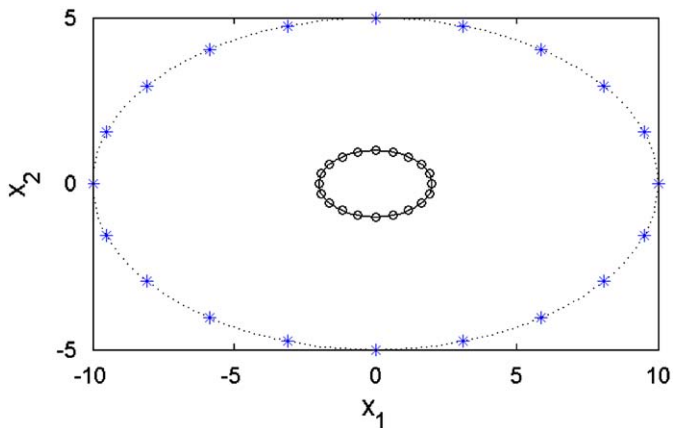


Fig. 1. Schematic illustration of boundary collocation points (o) on an ellipse domain (---) and source points (*) on the fictitious boundary (---).

origin. The accuracy variation of numerical results with respect to increasing number of collocation points, i.e. L , is shown in Fig. 2a. Roughly speaking, the accuracy of the numerical results first enhances with an increase of L , and then further increase of L would not gain much improvement in accuracy. It is observed that tens of collocation points (e.g. 24) suffice extreme accuracy. However, there are many oscillations, due to ill-conditioning of the interpolation matrix. The condition number $Cond$ of the interpolation matrix \mathbf{A}_{00} and $\mathbf{A}=(\mathbf{A}_{ij})$ is shown in Fig. 2b, where $Cond$ is defined as the ratio of the largest to the smallest singular value. This is also observed in other boundary-type techniques, such as the BKM and Trefftz method. There are several ways to mitigate the effect of bad conditioning, including the domain decomposition method [22], preconditioning technique based on approximate cardinal basis function, and the fast multiple method [23] and regularization methods such as the truncated singular value decomposition (TSVD) [24]. It is noted that in some cases presented below, the TSVD is necessary to obtain accurate results, and the truncation level is determined by the distinct gap in the singular value spectrum of the interpolation matrix \mathbf{A} .

The example is a standard benchmark problem in the BEM community, and it has previously been solved using the DR-BEM [10] and MR-BEM [12]. A comparison with the numerical results presented in these works [10,12] shows that the proposed method gives more accurate numerical solution with less computational effort.

In practical situations, the given data can always be approximated by piecewise polynomials, which will vanish after the operation of Laplace operator a few times. Therefore, the proposed method is expected to work for a wide range of practical problems.

Example 2. (Trigonometric forcing term) Now we consider a Poisson equation with trigonometric heat source subjected to mixed-type boundary conditions:

$$\begin{cases} \Delta u = 0.8\pi^2 \cos(\pi x_1), & (x_1, x_2) \in \Omega \\ \frac{\partial u}{\partial n} = 0, & (x_1, x_2) \in \Gamma_1 \\ u = 1 - 0.8\cos(\pi x_1), & (x_1, x_2) \in \Gamma_2 \end{cases} \quad (19a)$$

where the domain $\Omega = \{(x_1, x_2) | 0 < x_1 < 1, 0 < x_2 < 0.2\}$, and the two parts of the boundary $\Gamma_1 = \{(x_1, x_2) | 0 < x_1 < 1, x_2 = 0 \text{ or } 0.2\}$ and $\Gamma_2 = \{(x_1, x_2) | x_1 = 0 \text{ or } 1, 0 \leq x_2 \leq 0.2\}$. This example is taken from Ref. [12], and there is an error in the expression for the forcing term in Ref. [12].

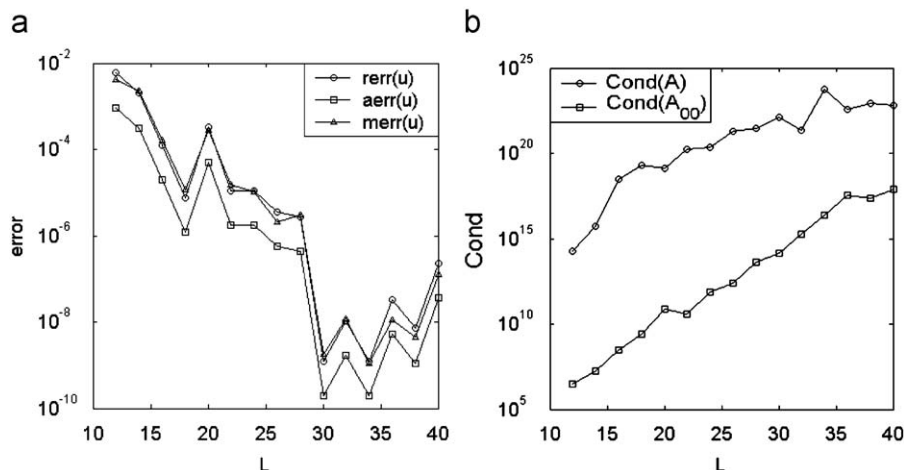


Fig. 2. (a) Numerical accuracy variation with respect to L and (b) the condition number of interpolation matrices.

The exact solution $u(x)$ is given by

$$u(x) = 1 - 0.8\cos(\pi x_1) \tag{19b}$$

For this example, the proposed method solves the following problem:

$$\begin{cases} (\Delta + \lambda^2)u = 0, & (x_1, x_2) \in \Omega \\ \frac{\partial u}{\partial n} = 0, & (x_1, x_2) \in \Gamma_1 \\ u = 1 - 0.8\cos(\pi x_1), & (x_1, x_2) \in \Gamma_2 \\ \Delta u = 0.8\pi^2 \cos(\pi x_1), & (x_1, x_2) \in \partial\Omega \end{cases} \tag{19c}$$

where the wave number λ is taken to be $\lambda = \pi$.

In the BPM with singular formulation, the source points are distributed evenly on a circle centered at the barycenter and with radius 10. The profile of the exact solution and error surfaces of the numerical solutions are displayed in Fig. 3. The accuracy of numerical results improves as the number of collocation points increases and tens of (e.g. 16) collocation points are sufficient for obtaining extremely accurate numerical results. When 12 and 16 boundary collocation points are used, the error surfaces are quite regular, and the maximum error appears to occur on the boundary adjacent to the corners. However, when 32 nodes are used, the error surface becomes quite irregular, and the errors seem to be quite uniform through the domain and its boundary. This also shows that the proposed method could work well with mixed-type boundary conditions. The observations from numerical results of Examples 1 and 2 seem still valid. It is to be noted that the problem has previously been solved using the MR-BEM [12], and the results presented here are far more accurate with the same number of collocation points.

Example 3. (Irregular geometry) We now consider the Helmholtz equation over an irregular domain, whose configuration is shown in Fig. 4.

$$\begin{cases} \Delta u + \lambda^2 u = x_1, & (x_1, x_2) \in \Omega \\ u = \sin(x_1) + \sin(x_2) + x_1, & (x_1, x_2) \in \partial\Omega \end{cases} \tag{20a}$$

where the wave number λ is taken to be 1. The analytical solution is given by

$$u = \sin(x_1) + \sin(x_2) + x_1 \tag{20b}$$

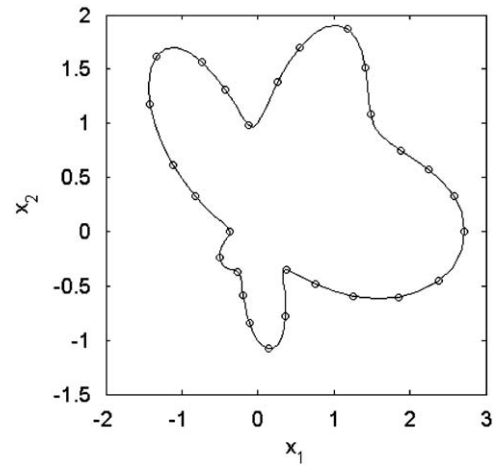


Fig. 4. Schematic illustration of the configuration of irregular domain for Example 3 and boundary collocation points (o).

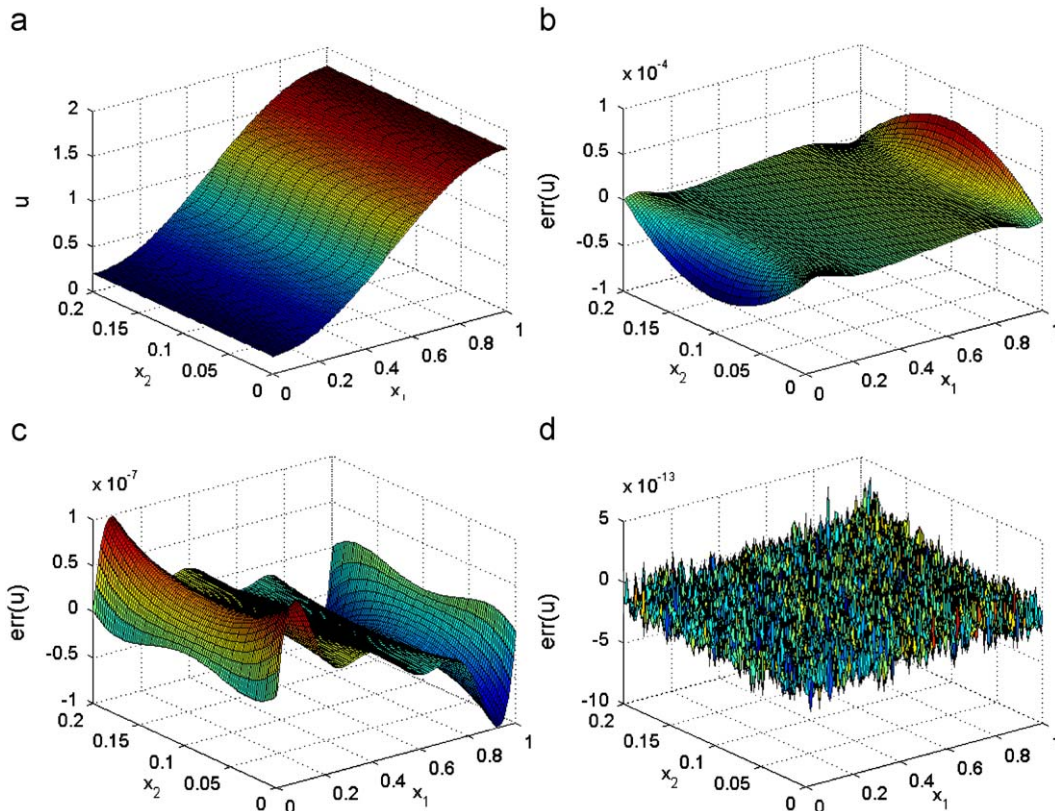


Fig. 3. Solution profile (a) of Example 2 and its error surfaces for the numerical results obtained using (b) 12, (c) 16, and (d) 32 collocation points.

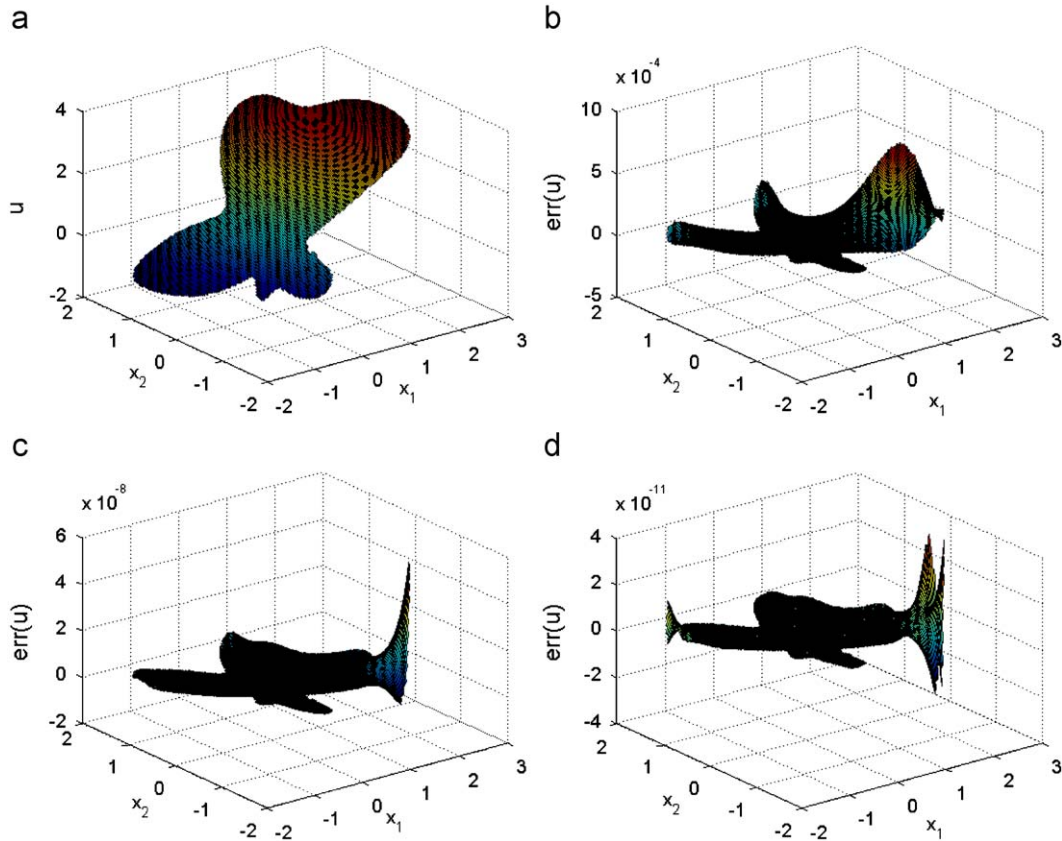


Fig. 5. Solution profile (a) of Example 3 and its error surfaces for the numerical results obtained using (b) 12, (c) 24, and (d) 32 collocation points.

For the present example, we have to solve the following elliptic partial differential equations

$$\begin{cases} \Delta(\Delta + \lambda^2)u = 0, & (x_1, x_2) \in \Omega \\ u = \sin(x_1) + \sin(x_2) + x_1, & (x_1, x_2) \in \partial\Omega \\ (\Delta + \lambda^2)u = x_1, & (x_1, x_2) \in \partial\Omega \end{cases} \quad (20c)$$

In the BPM with singular formulation, the source points are distributed on a circle centered at (0.5, 0.5) and with radius 10. The solution profile of the exact solution and error surfaces of the numerical solutions are shown in Fig. 5. It is observed that the results are comparable with that of foregoing examples, which shows that the proposed method works equally well over irregular geometries. The maximum error occurs at the boundary.

It is to be noted that the irregularity of the geometry does not entail singular solution. For problems involving singularities, special treatment is required, and it is deferred to future works.

From the numerical results for Examples 1–3 it can be observed that the proposed method can be very efficient for certain Poisson and Helmholtz problems, and it can give extreme accuracy that is rarely achievable for other methods without entailing very expensive computations.

In addition, three-dimensional problems are usually not easy to deal with by traditional numerical techniques partly because the computational complexity increases exponentially with dimensionality d . This effect has been dubbed the curse of dimensionality, and is one of the greatest barriers in higher-dimension computing. The following examples are intended to verify numerically the accuracy and efficiency of the present method for 3D problems. The 3D domain Ω is taken to be a cube

with all sides of equal length 2, i.e., $\Omega = [-1, 1]^3$, and the source points are distributed evenly on a sphere centered at the origin and with radius 5.

Example 4. (3D Poisson equation) Consider the following equation in the 3D case:

$$\begin{cases} \Delta u(x) = -2, & (x_1, x_2, x_3) \in \Omega \\ u(x) = -\frac{1}{3}(x_1^2 + x_2^2 + x_3^2), & (x_1, x_2, x_3) \in \partial\Omega \end{cases} \quad (21a)$$

This example is taken from Ref. [10], where it is solved using the DR-BEM. The analytical solution is given by

$$u(x, y, z) = -\frac{1}{3}(x_1^2 + x_2^2 + x_3^2) \quad (21b)$$

For this example, we have to solve the following problem

$$\begin{cases} \Delta^2 u(x) = 0, & (x_1, x_2, x_3) \in \Omega \\ u(x) = -\frac{1}{3}(x_1^2 + x_2^2 + x_3^2), & (x_1, x_2, x_3) \in \partial\Omega \\ \Delta u(x) = -2, & (x_1, x_2, x_3) \in \partial\Omega \end{cases} \quad (21c)$$

Numerical results for Example 4 obtained using various numbers of collocation points are shown in Table 1. The proposed method is found to work equally well for this 3D problem as in the previous 2D cases. The accuracy of the numerical results obtained using 54 nodes is comparable to that using DR-BEM with 48 BEM nodes and 27 internal nodes for the DRM [10]. This indicates that the proposed method may be a competitive numerical technique for higher-dimensional problems.

Example 5. (3D modified Helmholtz problem) Now we consider the following modified Helmholtz problem:

$$\begin{cases} \Delta u - \lambda^2 u = \frac{(3 - \lambda^2)}{\lambda^2} e^{x_1 + x_2 + x_3}, & (x_1, x_2, x_3) \in \Omega \\ u = \frac{1}{\lambda^2} e^{x_1 + x_2 + x_3}, & (x_1, x_2, x_3) \in \partial\Omega \end{cases} \quad (22a)$$

where λ is the wave number, and in the present study, it is taken to be $\lambda=20$. This example is taken from Ref. [25]. The exact solution to the problem is given by

$$u = \frac{1}{\lambda^2} e^{x_1 + x_2 + x_3} \quad (22b)$$

For this problem, the proposed method solves the following problem:

$$\begin{cases} (\Delta - k^2)(\Delta - \lambda^2)u = 0, & (x_1, x_2, x_3) \in \Omega \\ u = \frac{1}{\lambda^2} e^{x_1 + x_2 + x_3}, & (x_1, x_2, x_3) \in \partial\Omega \\ \Delta u - \lambda^2 u = \frac{(3 - \lambda^2)}{\lambda^2} e^{x_1 + x_2 + x_3}, & (x_1, x_2, x_3) \in \partial\Omega \end{cases} \quad (22c)$$

where k is another wave number and equals $\sqrt{3}$ for this example.

Table 1
Numerical results for Example 4 with various numbers of boundary collocation points.

L	rerr(u)	aerr(u)	merr(u)
24	4.2255e-3	9.2781e-3	1.0030e-2
54	6.6860e-4	1.4681e-3	2.1330e-3
96	3.4425e-6	7.5589e-6	1.7371e-5
150	2.4556e-7	5.3919e-7	1.8652e-6
216	1.8528e-8	4.0684e-8	1.2647e-7
294	1.2308e-8	2.7026e-8	1.7015e-7
384	9.3166e-10	2.0457e-9	8.7876e-9

Table 2
Numerical results for Example 5 using various numbers of boundary collocation points.

L	rerr(u)	aerr(u)	merr(u)
24	8.8254e-2	3.1180e-3	7.6422e-3
54	2.0374e-2	7.1980e-4	1.6365e-3
96	4.4942e-4	1.5878e-5	4.7064e-5
150	1.7055e-5	6.0256e-7	2.1875e-6
216	9.1986e-7	3.2498e-8	1.9908e-7
294	3.6936e-7	1.3049e-8	1.0112e-7
384	7.1847e-9	2.5383e-10	1.2833e-9

The numerical results for Example 5 obtained using various numbers of collocation points are presented in Table 2. This problem has been solved previously using the MFS in conjunction with DRM and compactly supported radial basis functions [25]. The comparison shows that the results presented here seem far more accurate. Also note that the accuracy of the numerical results for Example 5 is comparable to that of Example 4, as clearly shown in Tables 1 and 2.

It is stressed that compared with 2D problems, no extra coding effort is required for 3D cases except a single line for the definition of the distance variable. The proposed method demands neither mesh generation nor domain discretization, which is a considerable saving compared with mesh-based methods, and it does not require internal points in comparison with the popular DRM.

3.2. The BPM with nonsingular formulation

Till now, we consider only singular formulations using the BPM. In this section, we present numerical results obtained using the nonsingular formulation. For the convenience of comparison of the pros and cons of singular and nonsingular formulations, this subsection gives numerical results of several foregoing benchmark problems using the nonsingular formulation.

Example 6. Consider the Poisson's equation with a polynomial forcing term in Example 1. The basis functions $u_1^*(x)$, $u_2^*(x)$ and $u_3^*(x)$ to the differential operators $L_1=\Delta$, $L_2=\Delta$ and $L_3=\Delta$ in R^2 are, respectively, taken to be

$$\begin{cases} u_0^*(x) = \exp(-c(x_1^2 - x_2^2))\cos(2cx_1x_2) \\ u_1^*(x) = r^2\exp(-c(x_1^2 - x_2^2))\cos(2cx_1x_2) \\ u_2^*(x) = r^4\exp(-c(x_1^2 - x_2^2))\cos(2cx_1x_2) \end{cases} \quad (23)$$

where c is a shape parameter. The function $u_0^*(x)$ is taken from Hon and Wu [9], and it is easy to verify that $u_1^*(x)$ and $u_2^*(x)$ satisfy the biharmonic operator and tri-harmonic operators, respectively. Therefore, $u_1^*(x)$ and $u_2^*(x)$ are nonsingular analogues to higher-order fundamental solutions. The collocation points are distributed uniformly along the boundary, and the locations of source points coincide with those of collocation points.

The numerical results for Example 6 using various numbers of collocation points are shown in Fig. 6(a). The shape parameter c has a significant effect on accuracy of the numerical results, as in the case of multi-quadric and Gaussian, and it is taken to be 0.1 for this example. The accuracy of numerical results improves with an increase of L ; however, further increase of L deteriorates the

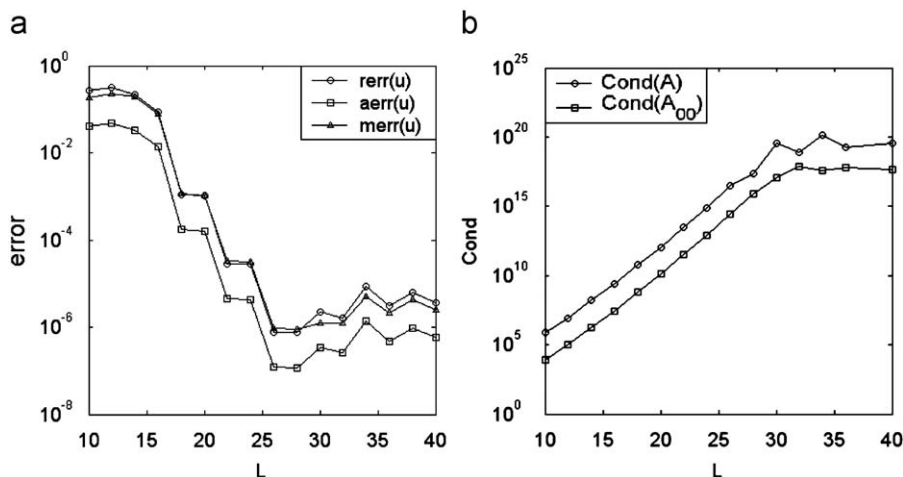


Fig. 6. (a) Numerical accuracy variation with respect to L and (b) the condition number of interpolation matrices.

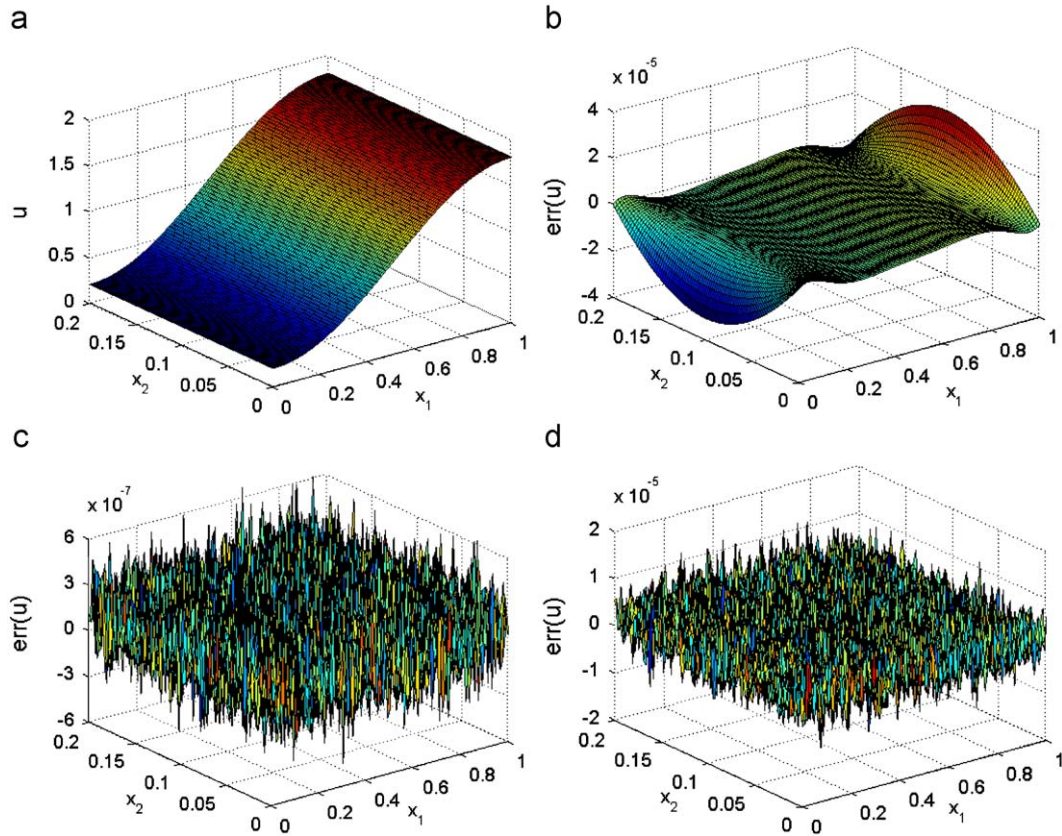


Fig. 7. Solution profile (a) of Example 7 and its error surfaces for the numerical results obtained using (b) 12, (c) 20, and (d) 28 collocation points.

accuracy slightly when it exceeds 28. The condition numbers of the interpolation matrices A and A_{11} are displayed in Fig. 6(b). It increases steadily with an increase of L , and then tends to level off. It is concluded that the nonsingular formulation also suffers from ill-conditioning.

Example 7. Consider the Poisson’s equation with a trigonometric forcing term in Example 2. Profile of the solution and error surfaces of the numerical solution for Example 7 are shown in Fig. 7, where the shape parameter c is taken to be 0.05. Accuracy of the numerical results first improves as L increases and then it does not gain much on increasing the boundary node number L . It is observed that the error surface for small numbers of collocation points is very smooth (e.g. $L=12$); however, it becomes highly oscillatory with more than 20 collocation points.

Example 8. Consider the 3D Poisson equation in Example 4. For 3D cases, we use the harmonic function of the 3D Laplacian equation, which can be intuitionally obtained as follows

$$H_3^0(x_{ik}, y_{ik}, z_{ik}) = \exp(-c(x_{ik}^2 - y_{ik}^2))\cos(2cx_{ik}y_{ik}) + \exp(-c(y_{ik}^2 - z_{ik}^2))\cos(2cy_{ik}z_{ik}) + \exp(-c(z_{ik}^2 - x_{ik}^2))\cos(2cz_{ik}x_{ik}) \quad (24)$$

Similarly, we can derive the harmonic function of m -order 3D Laplacian equation

$$H_3^m(x_{ik}, y_{ik}, z_{ik}) = r^{2m}\{\exp(-c(x_{ik}^2 - y_{ik}^2))\cos(2cx_{ik}y_{ik}) + \exp(-c(y_{ik}^2 - z_{ik}^2))\cos(2cy_{ik}z_{ik}) + \exp(-c(z_{ik}^2 - x_{ik}^2))\cos(2cz_{ik}x_{ik})\} \quad (25)$$

Numerical results for Example 8 using various numbers of collocation points are given in Table 3, where the shape parameter

Table 3
Numerical results for Example 8 with various numbers of boundary collocation points.

L	$rerr(u)$	$aerr(u)$	$merr(u)$
24	3.2484e-4	1.6895e-4	1.2136e-3
54	6.6860e-4	1.4681e-3	2.1330e-3
96	3.2484e-4	1.6895e-4	1.2136e-3
150	8.3461e-6	4.5497e-6	4.5950e-5
216	1.1365e-5	1.9788e-6	1.9125e-5
294	1.1694e-4	9.5855e-6	5.1803e-5
384	1.5480e-4	1.0625e-5	4.8512e-5
486	4.7847e-5	2.7641e-6	1.0930e-5

c is taken to be 0.1. The accuracy of the numerical results improves at the beginning with increasing boundary node number, then reaches a plateau, and starts oscillating with a further increase of boundary nodes.

From Table 3 and Figs. 5 and 6, it can be observed that the nonsingular formulation can also give accurate results for tested inhomogeneous problems.

4. Concluding remarks

In this paper, we elaborate on the numerical algorithm of boundary particle method in conjunction with recursive composite multiple reciprocity technique, which is a truly boundary-only, meshfree, and integration-free technique for inhomogeneous problems. Section 3 validates the efficacy, accuracy, and efficiency of the novel BPM and RC-MRM through various numerical experiments.

Ref. [16] shows that the present BPM in conjunction with recursive composite multiple reciprocity approach can be truly boundary-only for inhomogeneous PDE problems and appears promising to remedy singular integrations and costly domain integrals in the BEM and can be very efficient if the proper composite PDE is found. The boundary-only merit makes the present method far more attractive than the other existing numerical methods in handling some problems, for instance, inverse problems, where the boundary data in most cases are dominant in determining the systematic behavior and much more easily accessible than the inside-domain data.

It is stressed that for the general inhomogeneous term $f(x)$, we may find a suitable composite operator to reduce it to zero. If it is not workable in special cases, we can express it by a sum of polynomial or trigonometric function series, and then the present BPM can be simply implemented to solve these problems with the boundary-only discretization.

Acknowledgements

The work described in this paper was supported by a research project funded by the National Natural Science Foundation of China (Project no. 10672051).

Appendix A. Singular fundamental solutions and nonsingular general solutions

The basis functions employed in the iterative MRM satisfy the governing differential equation on the solution domain. They can be either singular fundamental solutions or nonsingular general solutions. Thus its practical applicability relies heavily on the availability of explicit expressions for fundamental, general, or harmonic solutions. For the convenience of the reader, we tabulate fundamental and general solutions to commonly used differential operators.

The fundamental solutions to commonly used differential operators are listed in Table A1 [17]. In the table, Δ denotes Laplacian, ∇ the gradient operator, λ a real number known as the wave number, v and r are the velocity vector and distance vector, respectively and r is the Euclidean norm between the point x and the origin. Furthermore, Y_0 and K_0 are the Bessel and modified Bessel functions of the second kind of order zero, respectively. Note that the fundamental solution to a differential operator is not unique. For the Laplacian, a constant may be included. However, it is often omitted as it does not have a significant effect on the accuracy of numerical results.

The nonsingular general or harmonic solutions to commonly used differential operators are listed in Table A2. In the table, I_0 and J_0 are the Bessel and modified Bessel functions of the first kind of order zero, respectively. The general solution for the 2D Laplace equation is taken from [9], where c is a shape parameter.

In the application of iterative MRM, higher-order fundamental and general solutions may be employed, which can be found in the MRM references. In the following, we will use higher-order

Table A1
Singular fundamental solutions of commonly used differential operators.

L	2D	3D
Δ	$-\frac{1}{2\pi} \ln r$	$\frac{1}{4\pi r}$
$\Delta + \lambda^2$	$\frac{1}{2\pi} Y_0(\lambda r)$	$\frac{\cos \lambda r}{4\pi r}$
$\Delta - \lambda^2$	$\frac{1}{2\pi} K_0(\lambda r)$	$\frac{e^{-\lambda r}}{4\pi r}$
$\Delta + v \cdot \nabla - \lambda^2$	$\frac{1}{2\pi} K_0(\mu r) e^{-v \cdot r/2}$	$\frac{e^{-\mu r}}{4\pi r} e^{-v \cdot r/2}$

Table A2
Nonsingular general or harmonic solutions of commonly used differential operators.

L	2D	3D
Δ	$\exp(-c(x_1^2 - x_2^2)) \cos(2cx_1x_2)$	$\exp(-c(x_1^2 - x_2^2)) \cos(2cx_1x_2) + \exp(-c(x_2^2 - x_3^2)) \cos(2cx_2x_3) + \exp(-c(x_3^2 - x_1^2)) \cos(2cx_3x_1)$
$\Delta + \lambda^2$	$J_0(\lambda r)$	$\frac{\sin(\lambda r)}{r}$
$\Delta - \lambda^2$	$I_0(\lambda r)$	$\frac{\sinh(\lambda r)}{r}$
$\Delta + v \cdot \nabla - \lambda^2$	$I_0(\mu r) e^{-v \cdot r/2}$	$\frac{\sinh(\mu r)}{r} e^{-v \cdot r/2}$

fundamental and general solutions to the Laplacian. The higher-order fundamental solution to the Laplacian is given by [12]

$$u^*(x) = \begin{cases} \frac{r^{2k} \ln r}{\pi}, & x \in R^2 \\ \frac{r^{2k-1}}{\pi}, & x \in R^3 \end{cases}$$

and its k th higher-order general solution is given by

$$u^*(x) = r^{2k} \exp(-c(x_1^2 - x_2^2)) \cos(2cx_1x_2), \quad x \in R^2.$$

Fundamental and general solutions to other differential operators can be found in Refs. [12,17,18]. In the present study, we confine our attention to the Laplacian- and Helmholtz-type operators. However, it is to be noted that their application to other differential operators commutative with the Laplacian, such as the convection-diffusion operator, would not pose any further difficulty.

References

- [1] Mukherjee YX, Mukherjee S. The boundary node method for potential problems. *Int J Numer Methods Eng* 1997;40:797–815.
- [2] Zhu T, Zhang JD, Atluri SN. A local boundary integral equation (LBIE) method in computational mechanics and a meshless discretization approach. *Comput Mech* 1998;21:223–35.
- [3] Li G, Aluru NR. Boundary cloud method: a combined scattered point/boundary integral approach for boundary-only analysis. *Comput Meth Appl Mech Eng* 2002;191:2337–70.
- [4] Maz'ya V. A new approximation method and its applications to the calculation of volume potentials. *Boundary point method*. In: 3. Kolloquium des DFG Forschungsschwerpunktes Randelementmethoden, 1991.
- [5] Fairweather G, Karageorghis A. The method of fundamental solutions for elliptic boundary value problems. *Adv Comput Math* 1998;9:69–95.
- [6] Chen CS, Cho HA, Golberg MA. Some comments on the ill-conditioning of the method of fundamental solutions. *Eng Anal Bound Elem* 2006 405–10.
- [7] Chen W. Symmetric boundary knot method. *Eng Anal Bound Elem* 2002;26:489–94.
- [8] Chen W, Tanaka M. A meshless, exponential convergence, integration-free, and boundary-only RBF technique. *Comput Math Appl* 2002;43:379–91.
- [9] Hon YC, Wu ZM. A numerical computation for inverse determination problem. *Eng Anal Bound Elem* 2000;24:599–606.
- [10] Partridge PW, Brebbia CA, Wrobel LW. *The dual reciprocity boundary element method*. Southampton: Computational Mechanics Publication; 1992.
- [11] Nowak AJ, Partridge PW. Comparison of the dual reciprocity and the multiple reciprocity methods. *Eng Anal Bound Elem* 1992;10:155–60.
- [12] Nowak AJ, Neves AC, editors. *The multiple reciprocity boundary element method*. Southampton: Computational Mechanics Publication; 1994.
- [13] Golberg MA, Chen CS, Bowman H, Power H. Some comments on the use of radial basis functions in the dual reciprocity method. *Comput Mech* 1998;21:141–8.
- [14] Cheng AHD. Particular solutions of Laplacian, Helmholtz-type, and polyharmonic operators involving higher order radial basis functions. *Eng Anal Bound Elem* 2000;24:531–8.
- [15] Sladek V, Sladek J. Multiple reciprocity method in BEM formulations for solution of plate bending problems. *Eng Anal Bound Elem* 1996 161–73.
- [16] Chen W. Meshfree boundary particle method applied to Helmholtz problems. *Eng Anal Bound Elem* 2002;26:577–81.
- [17] Kytke PK. *Fundamental solutions for differential operators and applications*. Boston: Birkhauser; 1996.

- [18] Chen W, Shen ZJ, Shen LJ, Yuan GW. General solutions and fundamental solutions of varied orders to the vibrational thin, the Berger, and the Winkler plates. *Eng Anal Bound Elem* 2005;29:699–702.
- [19] Zielinski AP, Herrera I. Trefftz method: fitting boundary conditions. *Int J Numer Methods Eng* 1987;24:871–91.
- [20] Li ZC, Lu TT, Huang HT, Cheng AHD. Trefftz, collocation, and other boundary methods—a comparison. *Numer Methods Partial Differential Equations* 2006;23:93–144.
- [21] Chen KH, Kao JH, Chen JT, Young DL, Lu MC. Regularized meshless method for multiply-connected-domain Laplace problems. *Eng Anal Bound Elem* 2006;30:882–96.
- [22] Kansa EJ, Hon YC. Circumventing the ill-conditioning problem with multi-quadric radial basis functions: applications to elliptic partial differential equations. *Comput Math Appl* 2000;39:123–37.
- [23] Beatson RK, Cherrie JB, Mouat CT. Fast fitting of radial basis functions: methods based on preconditioned GMRES iteration. *Adv Comput Math* 1999;11:253–70.
- [24] Hansen PC. Regularization tools: a Matlab package for analysis and solution of discrete ill-posed problems. *Numer Algorithms* 1994;6:1–35.
- [25] Golberg MA, Chen CS, Ganesh M. Particular solutions of 3D Helmholtz-type equations using compactly supported radial basis functions. *Eng Anal Bound Elem* 2000;24:539–47.